Numerical and Experimental Behaviour of Moment Resisting Connections using Blind Bolts within CFSHS columns

T. Pokharel, H.M. Goldsworthy

Department of Infrastructure Engineering, University of Melbourne, Parkville, 3010, Australia.

E.F. Gad

Faculty of Science, Engineering and Technology, Swinburne University of Technology, Hawthorn, 3122, Australia.

ABSTRACT: Concrete filled square hollow sections (CFSHS), comprising a square hollow section infilled with concrete have been used as a column in many structural applications in the USA, Europe, Japan and China. The CFSHS are not commonly used in Australia despite having many structural and constructional advantages. This is because it is perceived to be difficult/expensive to develop moment connections between open beams to the CFSHS. Welded connections are common in other countries but not common in Australia where shop welding and field bolting are the norm. The use of double-T blind bolted connections is proposed here as a structurally viable moment connection that satisfies the requirement for shop welding/field bolting and is easy to install. A detailed 3D finite element model has been developed of a sub-assemblage that consists of a concrete filled steel tube as the column, universal beams on opposite side of the column which are composite with a concrete slab and that are connected to the column with moment resisting blind-bolted connections. This model has been used to simulate the behaviour of a full scale sub-assemblage test in which gravity loads were applied followed by cyclic loading representing the effect of an earthquake. A satisfactory agreement was obtained between the FE model and experimental results.

1 INTRODUCTION

Large floor spans which provide open column-free spaces are usually preferred in buildings. For this purpose, moment resisting frames using CFSHSs as the columns have been popular in Japan, China and the USA for many years. The CFSHS columns have many advantages over RC or universal steel columns. However, their use has been limited in Australia and other countries due to difficulty in connecting them to beams. Welding is a common means to connect open beams to the CFSHS columns but in Australia welding is not preferred at site due to cost and quality control issues. Furthermore, in some past earthquakes, welded connections have sometimes not performed well under severe loading. In the Northridge earthquake, 1994, many rigid welded connections suffered premature brittle failure (SAC 1995).

Several researchers are trying to overcome the problems associated with the use of welded connections when connecting beams with the CFSHS columns. A number of blind bolted connections have been proposed [(France et al. 1999), (Pitrakkos and Tizani 2013), (Yao et al. 2008), (Agheshlui et al. 2015a), (Agheshlui et al. 2015b)] but there is not enough information to understand the behaviour of blind bolted connections under cyclic loading. This paper presents the experimental and numerical behaviour of moment resisting blind-bolted connections using headed anchored blind bolts (HABB). These connections were used in a sub-assemblage test conducted by (Agheshlui 2014) under cyclic loading at the University of Western Sydney. The overall behaviour under gravity and cyclic lateral loads of the internal sub-assemblage complete with beams on opposite sides of the CFSHS, blind bolted connections between the beams and CFSHS column, and a concrete slab on metal decking has been explained here.

2 EXPERIMENTAL SETUP

A typical 5 storey office building located in Melbourne was designed in accordance with Australian Standards (Standards-Australia 2007). The building was designed with CFSHS members as columns

and universal beam sections composite with the concrete slab as beams. The connections between composite beams and columns were moment resisting connections since they used blind bolts and T-stubs to connect both the top and bottom flanges of the beams to the CFSHS column. The perimeter frames are the main lateral load resisting members of the building. Thus, one of the perimeter connections was selected for the sub-assemblage test. Figure 1 shows the building plan for the case study building with the selected joints for the sub-assemblage test highlighted.

The full scale test was conducted with a 2.2m high CFSHS 400x400x12.5 as the column and 4.2m long 460UB82.1 composite with 140mm thick composite slab (i.e., RC slab composite with metal decking) on each side as shown in Figure 2. It was full-scale test and the details of the components are presented in Table 1. The test setup is shown in Figure 3. The slab width used represented the effective width at the connection region in accordance with Eurocode 4 (CEN 2004). It was placed symmetrically about the column for ease of construction.

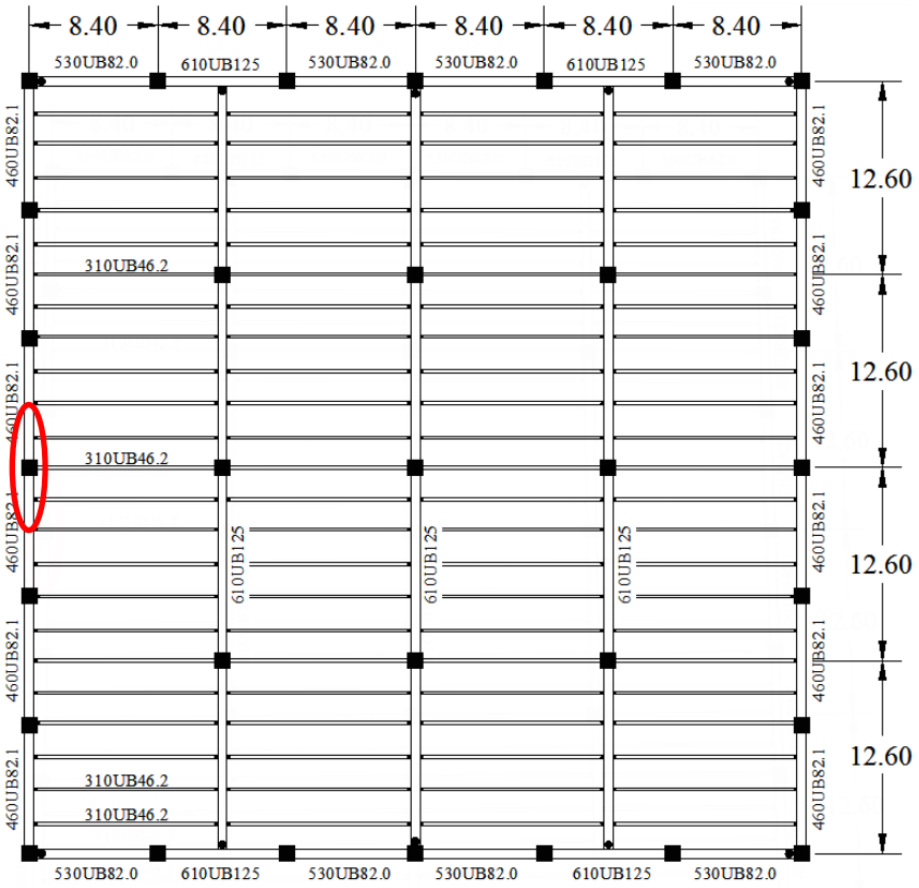

Figure 1: Building Plan with selected sub-assemblage highlighted (Agheshlui 2014).

The gravity loading was selected to replicate realistically the moment distribution in the beam in the connection region and the axial load in the column prior to the application of lateral loads. This is assumed to be the dead load plus 30% of live load as is usual in the loading combination that combines gravity and earthquake loading. An axial load of 1900kN was applied at the column and a gravity load of 150kN was applied to beam at a distance of 1.68m (which is 0.2L, L being the span between columns) on each side measured from the beam centre-line.

The gravity load was kept constant throughout the test. The cyclic displacement representing the effect of the lateral loads on the building was applied at the end of the beams. The displacement regime is given in Table 2.

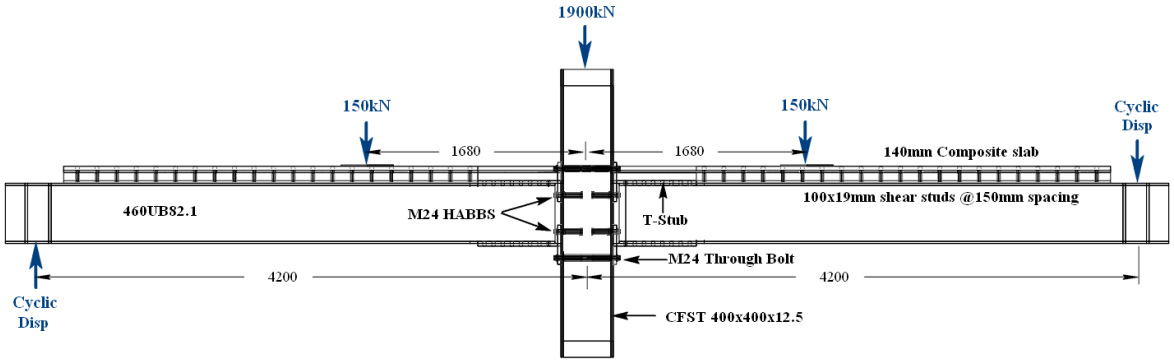

(a) Side View

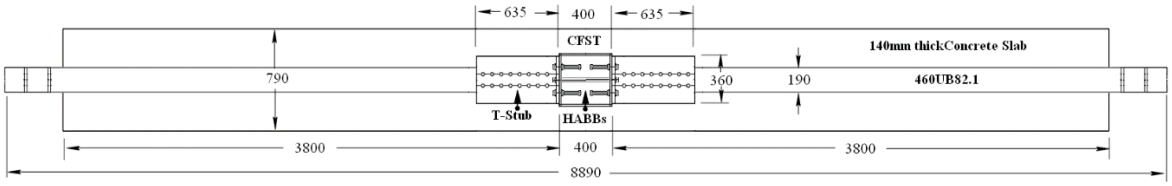

(b) Top View

Figure 2: Details of test specimen

Table 1: Details of sub-assemblage test components

S. No.	Component	Details
1	Column	400x400x12.5, 2.2m long, filled with 50 MPa concrete
2	Beams	460UB82.1, 4.2m long on each side, composite with the concrete slab
3	Slab	780mmx140mm, 8m long, 50MPa concrete
4	Condeck	1mm Condeck steel sheeting
5	Shear Studs	100x19 at 150mm spacing
6	Connections	Anchored blind bolted T-stub connections
7	Blind Bolts	PC 8.8 M24 HABB with 150mm extension
8	Through Bolt	PC 8.8 M24 placed in a steel pipe to isolate it from concrete
9	Rebar	Main Bar N20, Transverse Bars N16

Figure 3: Test Set-up

3 EXPERIMENTAL RESULTS

The load was applied in the experiment in different stages: first the gravity load of 1900kN at the column and then the 150kN loads on the beam at 1.68m away from the centerline of the CFSHS. Finally the equal and opposite cyclic displacements were applied at the end of beam. The results of the sub-assemblage test from the different stages are reported in detail in (Agheshlui 2014).

Table 2: Displacement details for the sub-assemblage test based on FEMA-461

Step	Amplitude (mm)	Number of cycles	Relative amplitude	Expected Status
1	7.0	2	0.068	Pre-yield
2	10.0	2	0.095	Pre-yield
3	14.0	2	0.133	Pre-yield
4	20.0	2	0.186	Pre-yield
5	28.0	2	0.260	Pre-yield
6	40.0	2	0.364	Post-yield
7	56.0	2	0.510	Post-yield
8	73.0	2	0.714	Post-yield
9	95.0	2	0.864	Post-yield
10	110.0	2	1.000	Estimated Failure
11	143.0	1	1.300	If does not fail in the previous step
Total No. Of steps		21		

Figure 4 shows the load vs displacement curve from the gravity load. The displacement in the figure was measured just under the gravity load application points in the beam.

Figure 5 shows the moment rotation behavior of one of the connections under the cyclic loading. The zero point in the figure is the position before applying any loads i.e., before the application of gravity loads.

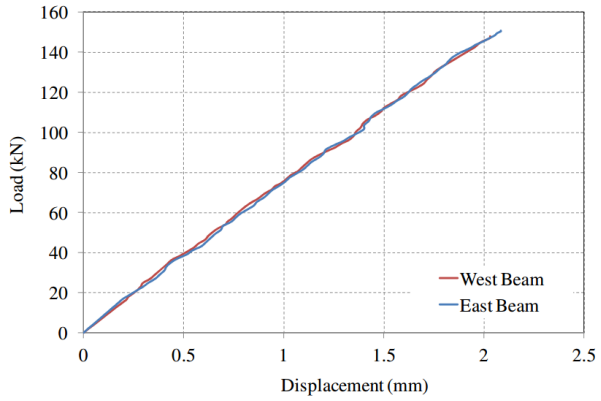

Figure 4: Load vs displacement of beam under gravity load

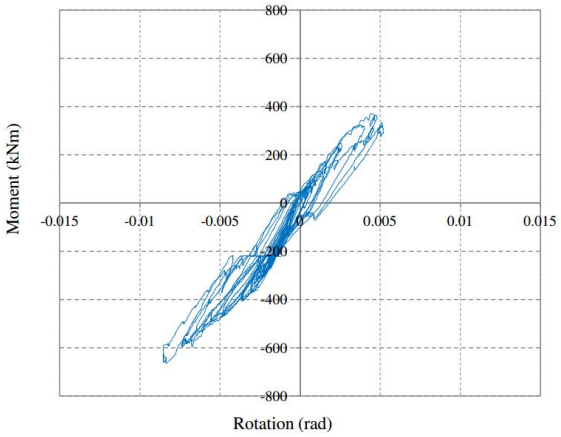

Figure 5: Connection moment rotation behavior

4 FINITE ELEMENT MODELLING

The purpose of this work is to create a FE model of the sub-assemblage test and validate the model with experimental results. By doing so, parametric studies can be done later using the verified model.

The rigorous FE model was developed using a 3D finite element program ABAQUS/Explicit. In this work, the Concrete Damage Plasticity (CDP) model was used to model the concrete as this model is ideal for cyclic loading. In the CDP isotropic damaged elasticity and multi-hardening plasticity are defined to describe irreversible damage (Abaqus 2012). For steel, a combined hardening model was used which considers the Bauchinger effect under cyclic loading.

4.1 *FE Model*

A three dimensional eight noded element (C3D8R) was used to model the concrete (slab and infill) and steel (steel tube, beam, T-Stub, bolts) to improve the rate of convergence of the explicit analysis. For the profiled steel sheeting, a four noded doubly curved shell element (S4R) was used. A two noded linear 3-D truss element (T3D2) was used for the rebar.

The complete test specimen shown in Figure 6 has following parts:

- Square Hollow Section (SHS 400x400x12.5) – 2.2 m long
- Concrete infill to SHS – M50
- Universal beam (460UB82.1) – 2 x 4m long
- Concrete Slab – M50 – (140mm thick)
- Condeck steel sheeting (1mm thick)
- Reinforcement (Embedded in concrete slab)
- T-Stubs – 4 Nos (Top and Bottom)
- M24 Through bolts – Bolt, Sleeve and Washer –2 Nos
- M24 Blind Bolts - Bolt, Sleeve and Washer – 4 Nos
- Shear Studs - 21 Nos (19mm dia studs at 150mm center to center spacing)

Here, a half of the test specimen was modelled as shown in Figure 6 because of the symmetry of the model. Figure 7 shows the FE representation of only a quarter of the model so the FE mesh can be clearly seen.

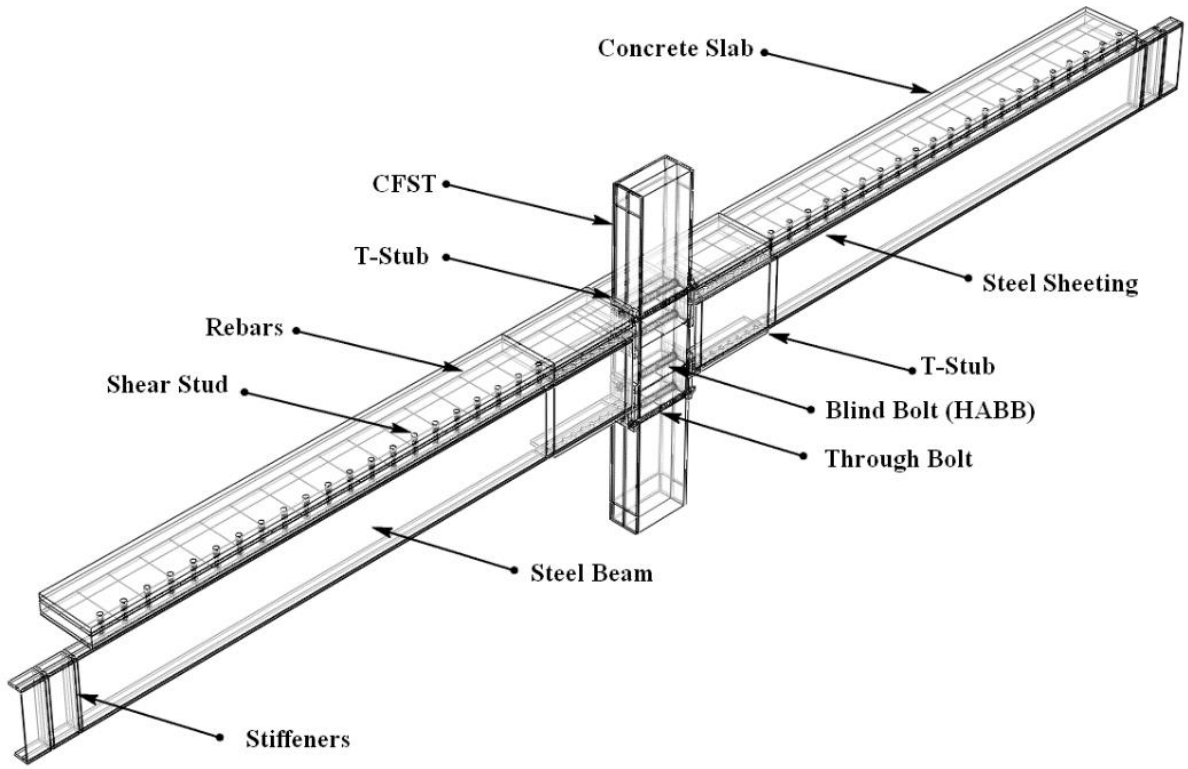

Figure 6: Symmetric half of the FE model

4.2 *Material Properties*

Coupon tests were conducted on material from the steel tube, beam, T-stub and threaded rods. Concrete compressive tests were conducted using standard cylinders. The mean 28 days compressive strength of concrete was found to be 46MPa. A summary of the material properties is listed in Table 3.

Table 3: Material Properties used in FE simulation

Material	Young's Modulus (MPa)	Yield Stress (MPa)	Ultimate Stress (MPa)	Source
Steel Tube	200,000	373	482	Coupon Test
Beam	210,000	348	484	Coupon Test
T-Stub	200,000	362	501	Coupon Test
Bolt	200,000	541	862	Coupon Test
Rebar	180,000	545	636	(Yao 2009)
Condeck	200,000	514	514	(Mirza and Uy 2011)

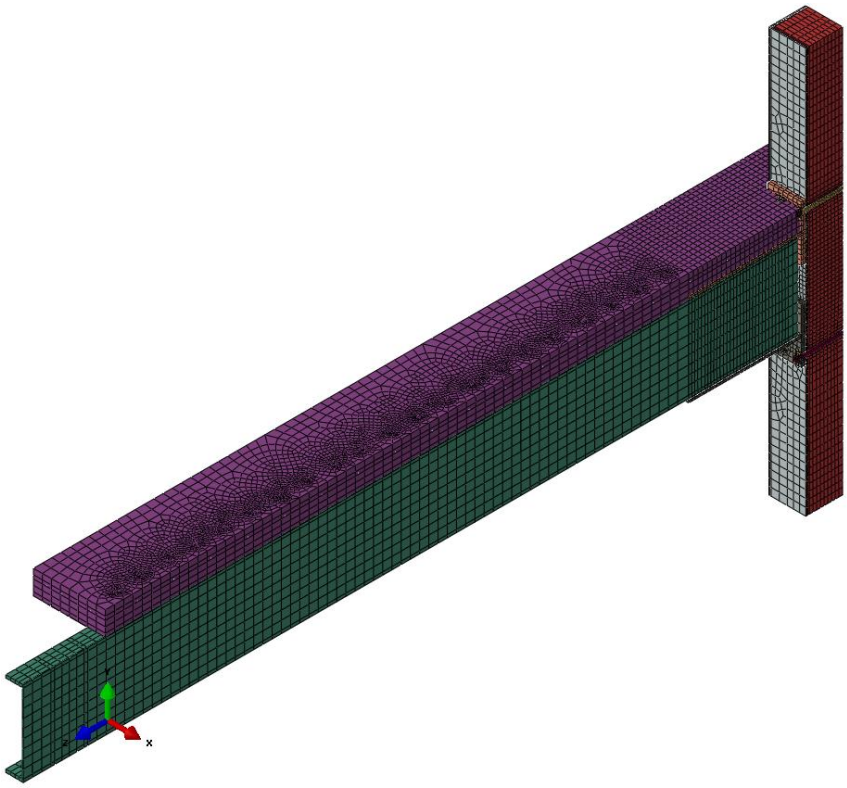

Figure 7: Symmetric quarter of the FE model with mesh

4.3 *Boundary Conditions*

Symmetric boundary conditions were applied along a vertical plane. The CFSHS column base was prevented from moving in the vertical direction and the horizontal direction. Similarly the horizontal displacement at the top of the CFSHS column was prevented as in the experimental program.

The rebar was modelled as a truss element and embedded constraints were applied with the concrete slab as the host region. The contact between different surfaces were considered. Hard contact along the normal direction and frictionless contact along the tangential directional were assumed unless otherwise specified.

A pre-tension force was applied to all bolts. The pre-tension was applied as a temperature load. The temperature of the bolt shank was lowered such that the length of bolt decreases creating compression forces in the connecting members. Several trials were performed to get the appropriate level of temperature to cause the desired tension in the bolts.

4.4 *Results of the FE analysis*

In this section the results of the FE simulation of the sub-assemblage test are presented and compared with the experimental results. The comparison is done in terms of either the force deformation relation or the moment rotation behaviour. The behaviour of different components of model are also compared.

As explained in the previous section the gravity load was applied to the column at the beginning and then to the beams. Figure 8 shows the load vs displacement curve at the point of applying the gravity load to the beams. The experimental result is also plotted in the same figure. Figure 9 shows the moment vs rotation curve at the same location. The FE results in both cases are in good agreement with the experimental results.

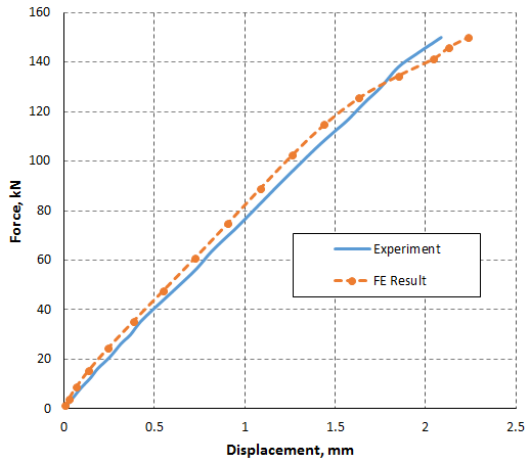

Figure 8: Force vs Displacement curve under gravity load

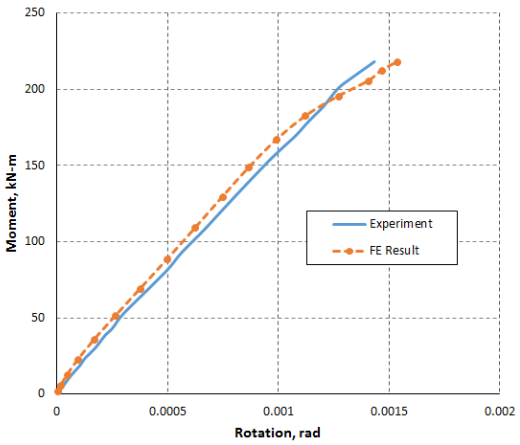

Figure 9: Moment vs Rotation curve under gravity load

After the gravity load, the cyclic displacement was applied in opposite directions at the end of the beams while keeping the gravity loads constant as in the experiment. Figure 10 shows the result of the analysis. The Load vs displacement curve from the FE analysis and the experimental result is compared in in this figure. As can be seen in the figure the capacity and stiffness of the connections at different cycles match well.

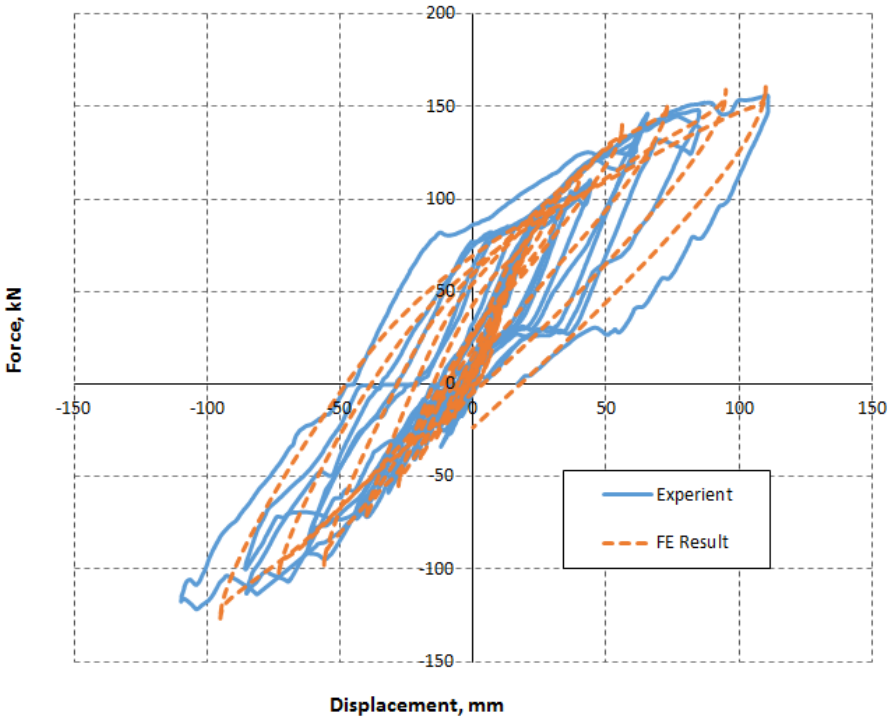

Figure 10: Cyclic load vs displacement curves

After few cycles of loading the concrete slab started to crack. Figure 11 shows the cracks in the slab after the 10th cycle during the experiment. The crushing of concrete can also be seen near the column. Similar cracking and crushing of the concrete in the slab was also obtained in the FE analysis. The cracking is shown in Figure 12 and the compressive crushing is shown in Figure 13. At this stage the crushing of concrete was concentrated at the top of the slab and the bottom of the slab was undamaged. The crushed region moved to the bottom end of the slab as the displacement in the beam end increased.

The reinforcement in the slab plays an important role in the connection especially in the earlier stage

i.e., before they yield. Figure 14(a) shows the strains in the reinforcement at the end of 10th cycle and Figure 14(b) shows the strains just after the main reinforcement yields.

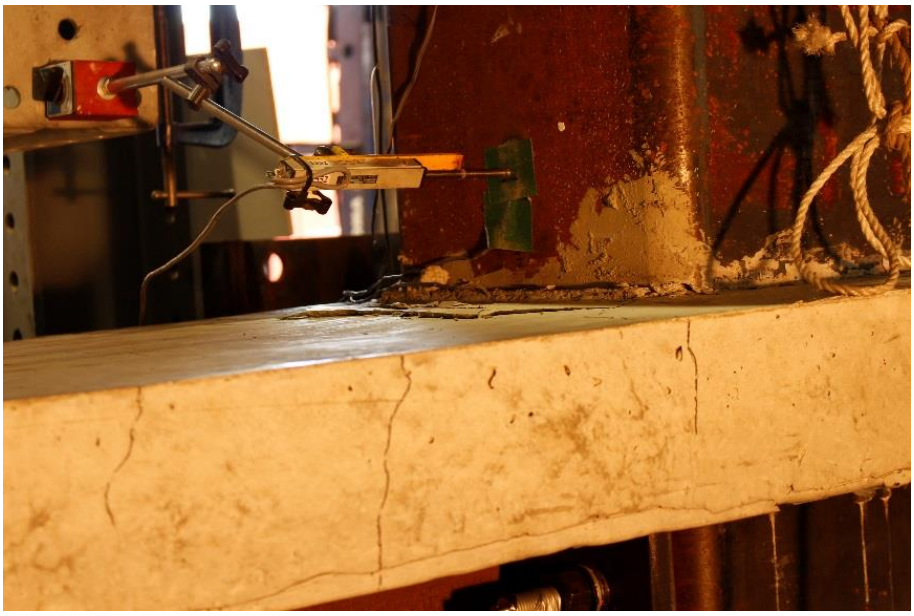

Figure 11: Cracks in slab in experiment

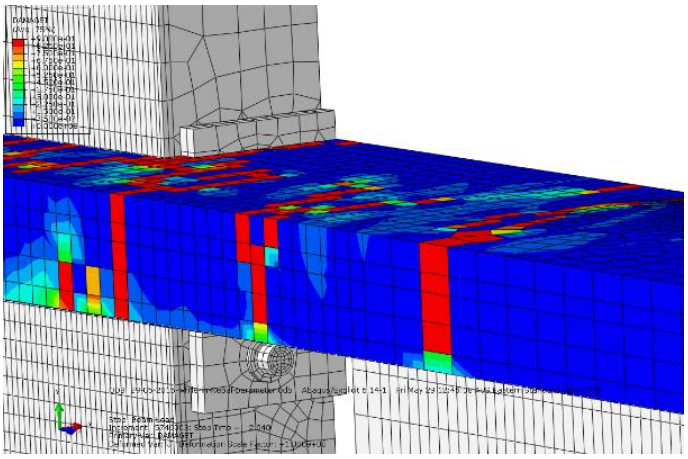

Figure 12: Cracks in slab after 10th cycles in FE simulation

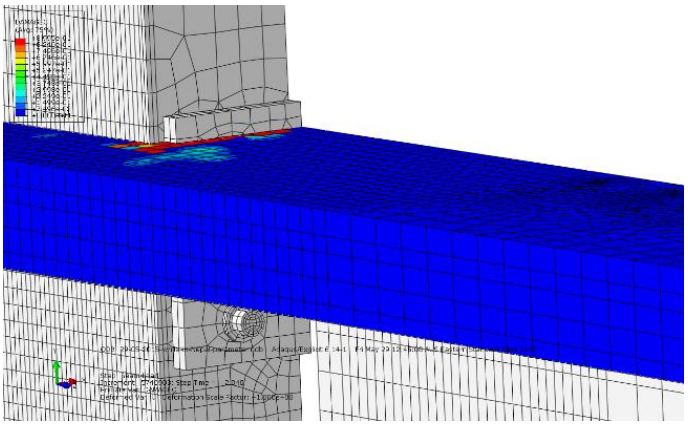

Figure 13: Compressive damage of concrete after 10th cycles in FE simulation

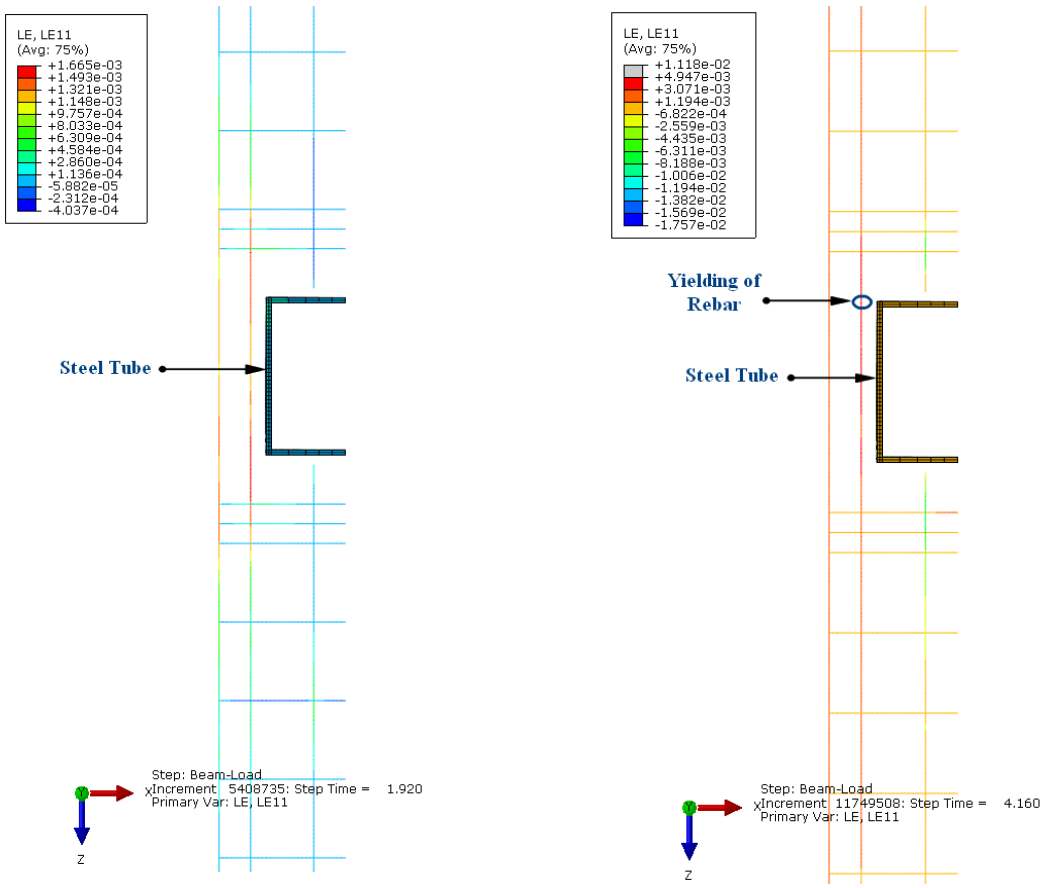

(a) (b)

Figure 14: Strain in slab reinforcement (a) at the end of 10th cycle and (b) just after the yield of the main rebar in tension in the FE with the location of first yielding

While designing the connection, plastic behavior in the connection was selected to be at the flange of T-Stubs to keep the bolts undamaged. The T-Stubs were designed to yield before load in the blind bolts reaches to 60% of their capacity. However, in the experiment, load in the bolts exceeded 60% of their capacity because the yield load of the T-flanges increased than expected. It was due to the underestimation of designed clamping forces applied to the bolts that provided fixity at the bolt lines (Agheshlui 2014). In the FE analysis, the flanges of T-Stub started to yield around the end of cyclic loading and bolt load reached near to their capacity.

5 CONCLUSION

The behaviour of an interior beam-column sub assemblage from a composite frame with blind bolted moment resisting connections between the beams and columns was simulated experimentally and numerically. Both gravity and earthquake loading were applied simultaneously. The load-displacement and moment-rotation behaviour at different stages were investigated. Good agreement was obtained between the experimental and numerical results.

The connection used in this study was a moment resisting connection using a double T-Stub arrangement to connect a composite beam to the CFSHS column. The beam was acting compositely with the floor slab with equally spaced shear studs. The behaviour of the top side of the connection was enhanced due the presence of the concrete slab and the reinforcement within the slab. Ultimately, the longitudinal reinforcement yielded which allowed the crack in the concrete to open up. The finite element result was successful in replicating the yielding of reinforcement and cracking and crushing of concrete. Furthermore, the ultimate capacities correlated well with experimental observations. The use of the finite element modelling has been validated and will be further extended to perform parametric analyses.

REFERENCES:

Abaqus (2012) *Abaqus User Manual*: Dassault Systems.

Agheshlui, H. (2014) *Anchored blind bolted connections within concrete filled square steel hollow sections*. Unpublished PhD, The University of Melbourne.

Agheshlui, H., Goldsworthy, H. and Gad, E. (2015a) Tensile Behaviour of Groups of Anchored Blind Bolts within Concrete Filled Steel Square Hollow sections. *Engineering Structures*.

Agheshlui, H., Goldsworthy, H., Gad, E. and Fernando, S. (2015b) Tensile behaviour of anchored blind bolts in concrete filled square hollow sections. *Materials and Structures*.

CEN (2004) Eurocode 4: Design of composite steel and concrete structures. *European Committee for Standardisation*.

France, J. E., Buick Davison, J. and A Kirby, P. (1999) Moment-capacity and rotational stiffness of endplate connections to concrete-filled tubular columns with flowdrilled connectors. *Journal of Constructional Steel Research, 50*(1), pp. 35-48.

Mirza, O. and Uy, B. (2011) Behaviour of composite beam–column flush end-plate connections subjected to low-probability, high-consequence loading. *Engineering Structures, 33*(2), pp. 647-662.

Pitrakkos, T. and Tizani, W. (2013) Experimental behaviour of a novel anchored blind-bolt in tension. *Engineering Structures, 49*, pp. 905-919.

SAC (1995) Interim Guidelines: Evaluation, Repair Modification and Design of Steel moment Frames. *FEMA-267*.

Standards-Australia (2007) AS 1170.4, structural design actions, part 4: Earthquake actions in australia. in,Sydney: Standards-Australia.

Yao, H., Goldsworthy, H. and Gad, E. (2008) Experimental and numerical investigation of the tensile behavior of blind-bolted T-stub connections to concrete-filled circular columns. *Journal of Structural Engineering, 134*(2), pp. 198-208.

Yao, H. J. (2009) *Moment-Resisting Beam-To-Circular Column Connection With Blind Bolts And Extensions*. Unpublished PhD, The University of Melbourne.